

Dual Energy X-ray Material Decomposition

I. Project Summary

Standard X-ray imaging brings difficulty for surgeons to identify region of interest (ROI) features from anatomical clutter. Dual energy X-ray enables anatomical clutter reduction via material decomposition by utilizing the physical properties of X-ray formulations. Fig.1 illustrates the decomposition process. Traditional Dual Energy X-ray Absorptiometry (DEXA) system has been developed in analyzing bone density, fat tissue, etc. But the model is largely approximated and simplified, because the target ROI is usually large and not targeted to small region accuracy. Thus, we propose to re-design the algorithm and improve the accuracy on decomposition of injected cement during femoroplasty. Decomposed frames can be used to improve 3D reconstruction of the injected cement, to better understand the cement distribution.

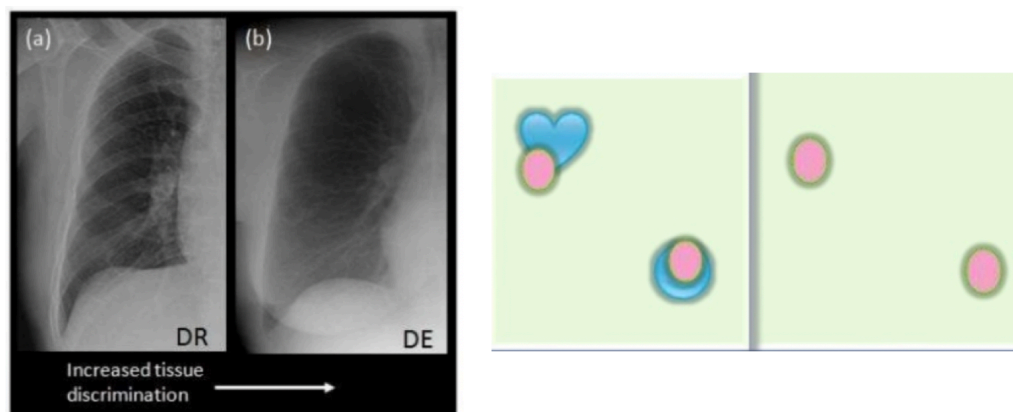


Figure 1. Illustration of material decomposition^[1].

II. Paper Selection

The paper selected for this review and critique is:

Adler, Jonas, and Ozan Öktem. "Learned primal-dual reconstruction." *IEEE transactions on medical imaging* 37.6 (2018): 1322-1332.

This paper proposed a novel method on improving low dose computed tomography (CT) reconstruction. Its key innovation is combining model driven approach and data driven approach for solving ill-posed inverse problems. The reconstruction application is not directly related to the dual energy decomposition, but the method is highly generalizable to related ill-posed inverse problems in image modalities. From this prospective, dual energy X-ray decomposition is exactly trying to solve an ill-posed inverse problem between acquisition domain and decomposition domain. Thus, this proposed method has realistic significance in our project.

III. Summary and Key Result

In summary, this paper proposed an algorithm of learning based iterative reconstruction. It gives state-of-the-art results on computed tomography problem for both analytical and human phantoms. The study comprehensively conducts ablation studies on related methods, including Filtered Back Projection (FBP) [2] and Total Variation (TV) [3], U-net denoising [4] and other simplified Primal-Dual algorithms. The proposed method reaches the best performance in the metric of peak signal to noise ratio (PSNR) and structural similarity index (SSIM). Fig. 2 illustrates the CT reconstruction performance using traditional FBP method and the proposed Primal-Dual algorithm.

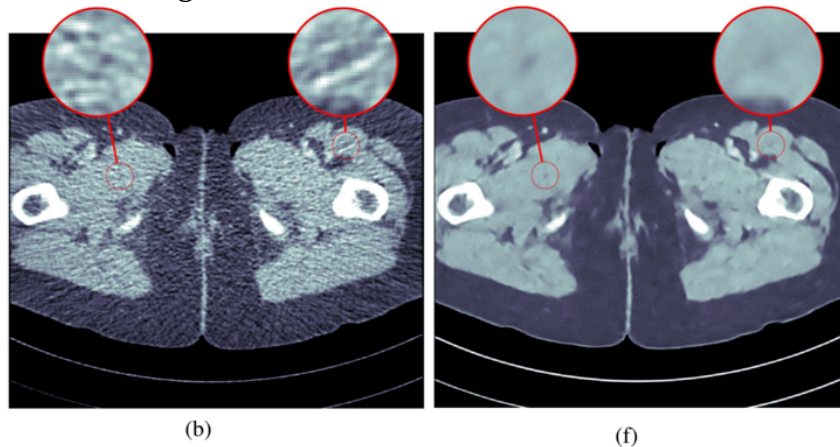


Figure 2. Reconstructions of a human phantom. (b) Filtered back projection (FBP). (f) Primal-Dual algorithm.

IV. Significance

Significance of this paper lies in the following several aspects:

- It largely out performs the classical schemes (FBP^[2] and TV^[3]) as referred in the previous section.
- It also significantly improves over the previous end-to-end deep learning based methods, such as U-Net^[4] based post-processing and learned gradient method^[5]. PSNR improvement exceeds 6dB.
- It inspires related and future research in Learned Primal-Dual schemes and that the method will be applied to other imaging modalities.

V. Necessary Background

This research is built upon fundamental math derivations. First, the author formulates the inverse problem as

$$g = \mathcal{T}(f_{true}) + \delta g ,$$

Where $f_{true} \in X$ is in the primal domain; $g \in Y$ is in the dual domain. δg is the noise component of the data. (Note: here the definition of primal and dual domain is different from the gradient based convention. The critique will follow the author's definition).

In the scenario of CT reconstruction, the primal domain is the 3D reconstruction; dual domain is the 2D projections. Considering our application in X-ray decomposition, our decomposed data $T(\mathbf{u})$ is essentially the primal and X-ray measurements $M(\mathbf{u})$ are the dual. Our formulation of this inverse problem is

$$\begin{aligned} m(\mathbf{u})_L &= w_L^1 T^1(\mathbf{u}) + w_L^2 T^2(\mathbf{u}) \\ m(\mathbf{u})_H &= w_H^1 T^1(\mathbf{u}) + w_H^2 T^2(\mathbf{u}), \end{aligned}$$

Where $m(\mathbf{u})$ is the measurement at each pixel \mathbf{u} . w is the coefficients and $T(\mathbf{u})$ is the desired decomposition “thickness”.

For the traditional model driven approach, it is essentially solving an optimization objective function:

$$\min_{f \in X} L(T(f), g).$$

But the problem is that it is highly possible to overfit against training data. Therefore, what people usually do is adding a regularization functional $S(f)$. Then the optimization function looks like

$$\min_{f \in X} [L(T(f), g) + \lambda S(f)]. \lambda \geq 0$$

In our application of X-ray decomposition, our objective function is essentially solving a least square problem:

$$\min_{T(\mathbf{u})} (M(\mathbf{u}) - WT(\mathbf{u}))^T (M(\mathbf{u}) - WT(\mathbf{u}))$$

Our preliminary results have shown that this is likely to cause the negative $T(\mathbf{u})$ problem, which violates physical constraints. Thus, we changed our objective to be constrained least square solution for decomposition:

$$\min_{T(\mathbf{u})} (M(\mathbf{u}) - WT(\mathbf{u}))^T (M(\mathbf{u}) - WT(\mathbf{u})), \text{ constrained to } T(\mathbf{u}) \geq 0$$

In order to solve the aforementioned objective function, traditional methods are basically gradient based methods, such as gradient descent or high order gradient descent (Newton methods). But, when the function itself is non-differentiable, there is an alternative way, which is primal dual hybrid gradient (PDHG) algorithm [6]. Table.1 displays the algorithm pipeline. Basically, it updates the variable in primal and dual space iteratively to overall minimize the objective function. This method brings the opportunity to implement a complex multi variable optimization process in an iterative way. The proximal operator marked in this algorithm as $prox_{\tau G}(f)$ is an alternative way to calculate gradient when the function itself is non-smooth.

Algorithm 1 Non-Linear primal dual hybrid gradient

- 1: Given: $\sigma, \tau > 0$ s.t. $\sigma \tau \|\mathcal{K}\|^2 < 1$, $\gamma \in [0, 1]$ and $f_0 \in X$, $h_0 \in U$.
 - 2: **for** $i = 1, \dots$ **do**
 - 3: $h_{i+1} \leftarrow \text{prox}_{\sigma \mathcal{F}^*}(h_i + \sigma \mathcal{K}(\bar{f}_i))$
 - 4: $\bar{f}_{i+1} \leftarrow \text{prox}_{\tau \mathcal{G}}(f_i - \tau [\partial \mathcal{K}(f_i)]^*(h_{i+1}))$
 - 5: $f_{i+1} \leftarrow \bar{f}_{i+1} + \gamma (f_{i+1} - \bar{f}_{i+1})$
-

Table 1. Primal dual hybrid gradient (PDHG) algorithm

This corresponds to our design of optimization model for the decomposition process. We can do the same alternative update for physical model and the residual regularization term. Fig. 3 illustrates this process.

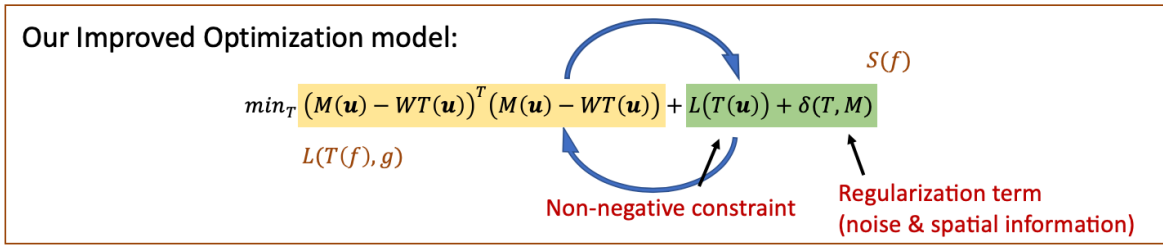


Figure 3. Illustration of our iterative optimization process.

VI. Contributions

Starting from the idea of PDHG algorithm. The innovation is introducing deep learning to replace the proximal operator by a network. This design is then called “Learned PDHG algorithm”. Table. 2 displays the details of this learned PDHG algorithm. The operator Γ_θ and Λ_θ are called learned proximal, which simply notes the learning part.

Algorithm 2 Learned PDHG

- 1: Initialize $f_0 \in X, h_0 \in U$
 - 2: **for** $i = 1, \dots, I$ **do**
 - 3: $h_{i+1} \leftarrow \Gamma_{\theta^d}(h_i + \sigma \mathcal{K}(\bar{f}_i), g)$
 - 4: $f_{i+1} \leftarrow \Lambda_{\theta^p}(f_i - \tau [\partial \mathcal{K}(f_i)]^*(h_{i+1}))$
 - 5: $\bar{f}_{i+1} \leftarrow f_{i+1} + \theta(f_{i+1} - f_i)$
 - 6: **return** $f_I^{(1)}$
-

Table 2. Learned PDHG algorithm

Based on this pipeline, the author further improves by introduce “memory” between iterations. Then it gets to the idea of Learned Primal-Dual algorithm. Fig.3 displays the details of this learned primal-dual algorithm.

Algorithm 3 Learned Primal-Dual

- 1: Initialize $f_0 \in X^{N_{\text{primal}}}, h_0 \in U^{N_{\text{dual}}}$
 - 2: **for** $i = 1, \dots, I$ **do**
 - 3: $h_i \leftarrow \Gamma_{\theta^d}(h_{i-1}, \mathcal{K}(f_{i-1}^{(2)}), g)$
 - 4: $f_i \leftarrow \Lambda_{\theta^p}(f_{i-1}, [\partial \mathcal{K}(f_{i-1}^{(1)})]^*(h_i^{(1)}))$
 - 5: **return** $f_I^{(1)}$
-

Table 3. Learned Primal-Dual algorithm.

This idea is inspirational to our material decomposition pipeline. We can also bring this insight to our design by learning the updates of the variables in primal/dual domain using a convolutional network. Fig. 4 displays a sketch to our pipeline design.

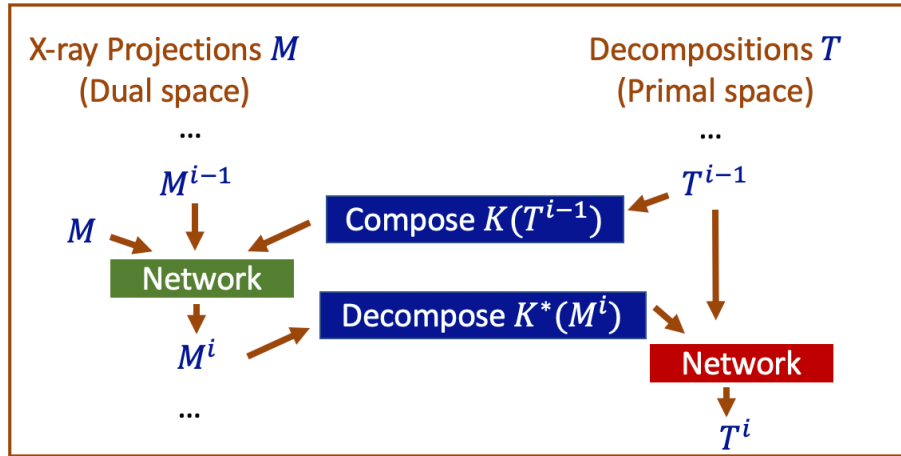


Figure 4. Sketch of our modified pipeline.

Fig.5 is the implementation detail of the network structure. The right blue and red box stacks are actually the implementation of the iterative update. The left two detailed structured boxes are the learning architecture of the dual and primal update. The light blue reflects the convolutional operation that maps the inputs to the update prediction. The “add” operation actually adds the current status with the updates to the next stage, which reflecting that the network is essentially learning the update.

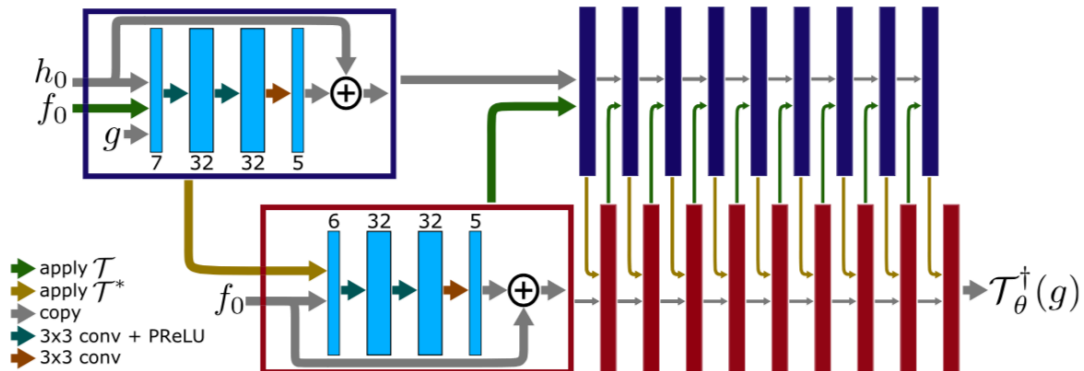


Fig. 2. Network architecture used to solve the tomography problem. The dual iterates are given in blue boxes, while the primal iterates are in the red boxes. The blue/red boxes all have the same architecture, which is illustrated in the corresponding large boxes. Several arrows pointing to one box indicates concatenation. The initial guesses enter from the left, while the data is supplied to the dual iterates. In the classical PDHG algorithm, the primal iterates would instead of a CNN be given by $\text{prox}_{\mathcal{T}}g$ with over-relaxation, and the dual iterates would be given by $\text{prox}_{\mathcal{T}^*}$.

Figure 5. Network Implementation.

VII. Experiment

The author conducts experiments using 1) ellipse phantoms and 2) human phantoms. For the phantom experiment, training data is randomly generated ellipses on a 128×128 pixel domain. The forward operator is the ray transform $T = P$, and the back-projection is $[\partial T(f)]^* = P^*$. The projection geometry was a sparse 30 view parallel beam geometry. Validation is then using a standard reconstruction phantom data, which is shepp-Logan phantom.

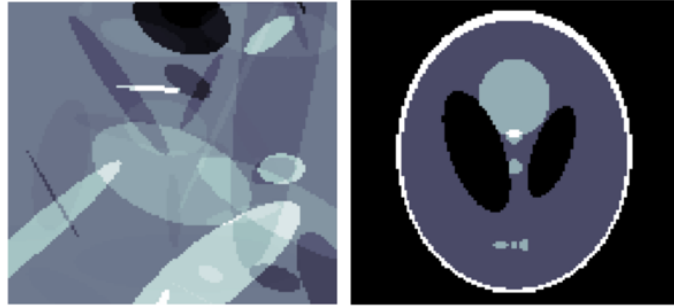


Figure 6. Left: random ellipses. Right: Shepp-Logan phantom.

The author also conducts experiments on real acquired CT scans. 10 patient full dose CT scans were acquired, of which 9 are used for training, 1 is left for evaluation. Reconstruction slice thickness is 3 mm, resulting in 2,168 training images. Projection geometry is two-dimensional fan-beam geometry with 1,000 angles. Non-linear forward model is given by Beer-Lamberts law $T(f)(l) = e^{-\mu P(f)(l)}$, while the adjoint of the derivative is $[\partial T(f)]^*(g) = -\mu P^* \left(e^{-\mu P(f)(\cdot)} g(\cdot) \right)$ for $g \in Y$.

VIII. Results

The author compares several widely used algorithms, including standard Filtered back-projection (FBP)^[2] and (isotropic) TV regularized reconstruction^[3]. Data-driven methods are also included in comparison. The comparison is against a deep learning based approach for post-processing based on a U-Net^[4] structure. The Learned Gradient method^[6] is similar to the algorithm proposed in this article, but it learns the update of the gradient based method. Table I summarizes the results using the metric: peak signal to noise ratio (PSNR) and SSIM (structural similarity index) and runtime. Clearly the proposed learned Primal-Dual algorithm reaches the best performance considering PSNR and SSIM. Traditional method FBP has the least runtime because it is not running iteratively.

TABLE I

COMPARISON OF RECONSTRUCTION METHODS FOR THE ELLIPSES.
PSNR MEASURED IN dB AND RUNTIME IN ms

Method	PSNR	SSIM	Runtime	Parameters
FBP	19.75	0.597	4	1
TV	28.06	0.929	5 166	1
FBP + U-Net denoising	29.20	0.944	9	10^7
FBP + residual denoising	32.38	0.972	9	$1.2 \cdot 10^5$
Learned Gradient	32.29	0.981	56	$1.2 \cdot 10^4$
Learned PDHG	28.32	0.909	48	$2.4 \cdot 10^4$
Learned Primal	36.97	0.986	43	$1.2 \cdot 10^5$
Learned Primal-Dual	38.28	0.989	49	$2.4 \cdot 10^5$

Table II summarizes the performance in the CT phantom study. The difference between linear and non-linear is the implementation of forward projector for runtime concern. In the real CT scan, we can still see that the proposed method reaches the best performance.

TABLE II
COMPARISON OF THE LEARNED PRIMAL-DUAL ALGORITHM WITH
OTHER METHODS FOR THE HUMAN PHANTOM DATA. UNITS
FOR ENTRIES ARE THE SAME AS IN [TABLE I](#)

Method	PSNR	SSIM	Runtime	Parameters
FBP	33.65	0.830	423	1
TV	37.48	0.946	64 371	1
FBP + U-Net denoising	41.92	0.941	463	10^7
Learned Primal-Dual, linear	44.11	0.969	620	$2.4 \cdot 10^5$
Learned Primal-Dual, non-linear	43.91	0.969	670	$2.4 \cdot 10^5$

IX. Conclusion

In summary, the paper proposed an innovative method solving tomographic reconstruction problem. The algorithm is inspired by the PDHG algorithm, but replacing the proximal operators by learned operators. This proposed algorithm gives state of the art results in both phantom and human phantom study. This study also inspires future and related research to combine model-driven and learning based approaches to do optimization.

X. Assessment & Future improvement

Good:

- a. This is a very well-written and solid paper by combining the knowledge of frontier math and deep learning.
- b. Ablation studies and comparisons cover a wide range of related classical and learning based algorithms. Results and performance are analyzed in detail.
- c. It inspires related research of introducing learning in general inverse problems.

Improvement:

- a. Overfitting. Both phantom study and human CT study are conducted on limited data source or variants. The author didn't discuss too much on how to avoid overfitting. By training on 9 CTs, it doesn't mention the generalization ability to other CT samples, since the evaluation is only using 1 CT.
- b. Optimization still runs in an iterative way. The PDHG algorithm is useful in solving non-differentiable functions or complex functions, but for the easier or more straightforward dual/primal projection, it is possible to combine learning based and model based methods in a single optimization object, which will make the process more compact and likely get better performance.

XI. Reference

[1] Slide: Dual energy imaging and digital tomosynthesis: Innovative X-ray based imaging technologies, University of Toronto.

[2] Lauritsch, Günter, and Wolfgang H. Härer. "Theoretical framework for filtered back projection in tomosynthesis." *Medical Imaging 1998: Image Processing*. Vol. 3338. International Society for Optics and Photonics, 1998.

- [3] Osher, Stanley, et al. "An iterative regularization method for total variation-based image restoration." *Multiscale Modeling & Simulation* 4.2 (2005): 460-489.
- [4] Ronneberger, Olaf, Philipp Fischer, and Thomas Brox. "U-net: Convolutional networks for biomedical image segmentation." *International Conference on Medical image computing and computer-assisted intervention*. Springer, Cham, 2015.
- [5] J. Adler and O. Öktem, "Solving ill-posed inverse problems using iterative deep neural networks," *Inverse Problems*, vol. 33, no. 12, p. 124007, 2017.
- [6] A. Chambolle and T. Pock, "A first-order primal-dual algorithm for convex problems with applications to imaging," *J. Math. Imag. Vis.*, vol. 40, no. 1, pp. 120–145, 2011.